ICSV 17
THE 17th INTERNATIONAL CONGRESS ON SOUND & VIBRATION
CAIRO 18 - 22 JULY, 2010

POWER HARVESTING USING PIEZOMATERIAL IN A HELICOPTER ROTOR BLADE

P H de Jong, A de Boer, R Loendersloot, P J M van der Hoogt

Faculty of Engineering Technology, University of Twente, Enschede, the Netherlands,
e-mail: p.h.dejong@utwente.nl

Current power harvesting research has focused on bending beams and determining power output under a given excitation. For the European *CleanSky – Green Rotor Craft* project a tool is being developed which optimizes the piezoelectric material and placement thereof for power harvesting. It focuses on beam-like structures exhibiting more complex dynamics where the optimum configuration is not evident. In particular helicopter rotor blades are considered where strains are high and frequencies low, stepping away from typical high frequency / low strain harvesting applications. This application will allow for smart rotor blades, alleviate rotor induced vibrations, subsequently increasing comfort and possibly airframe longevity.

First an uncoupled model was developed, using an airfoil shape and vibration input from industry. The blade surface is covered with piezo electric patches of which the strain during one cycle is calculated. Materials, either ceramic or piezo polymer, are selected based on a peak strain criterion and the energy of each patch is then evaluated using a specified harvesting circuit. Optimum locations are determined using a minimum desired efficiency relative to the best performing patch. For aircraft application the main performance indicator is clearly the power to weight ratio.

Experiments have also been conducted which confirm the piezo polymer performance up in the percentage strain range where piezo ceramics fail. The harvesting performance of ceramic patches has also been evaluated. Measurements will be conducted on a complex beam shape to confirm the theoretical results as well when the theoretical model is completed.

Future development encompasses dynamic coupling since the behaviour may be influenced as more energy is extracted. An iteration algorithm will need to be selected for the optimization process. Lastly electrical models will be included as this directly determines the harvesting efficiency. The final tool will be applicable on any slender structure which exhibits complex harmonic loading.

1. Introduction

In the past few years power harvesting has gathered much interest with research being done in various directions. Conceptual practical applications have been developed by [1–3] varying from

modified backpacks to harvesting from the pitch links in rotorcraft.

On the materials side comparisons between various materials and construction has been researched as well. A comparison is made in [4] between monolithic PZT, an MFC and a PVDF patch [3] and [5] compare PZT in various constructions and conclude that interdigitated electrodes are detrimental to performance of the material.

A third field is the development of electrical circuits used to control and boost energy output. Impedance matching is the best known and most researched circuit. For example [6–8] investigate and optimize various parameters to improve harvesting efficiency and [9] provides an extensive derivation of the dynamics of harvesting systems utilizing this technique. More advanced techniques employing highly non-linear methods are [10] which only discharge the element at voltage peaks and [11] further optimizes the circuit. [12] developed a technique which inverts the piezo voltage upon strain maxima, significantly boosting piezo voltage and thereby energy output.

Within the framework of the European *CleanSky – Green Rotor Craft* project the application of power harvesting in the main rotor of rotorcraft to power smart systems is being investigated. Current research typically involves a sinusoidally excited beam for model validation purposes, e.g. [10–13]. A piezo element is fixed near the base where the deformations are the largest. For a rotor blade the optimal placement is unclear: low frequencies show large deformations and vice versa. On the other hand harvested power is roughly proportional to frequency and deformation squared. Significant coupling may also lead to attenuation of vibrations, limiting output.

This paper presents some initial steps towards a method which can be used to optimize the location of piezoelectric material on a beam experiencing complex loading/deformation. In section 2 two linear equations of motion (impedance matching and synchronous electric charge extraction – SECE) are derived which govern the vibration of a 1 DOF system for a sinusoidal input. These may be used in an iterative calculation for optimization of piezo patches in highly coupled structures. The non-linear equations related to power harvesting result in great computational difficulty in case of coupling and are unsuitable for optimization routines. In section 3 the validity of the equation of motion for the SECE system is investigated for more complex excitations.

2. Substitution of hysteretic damping for piezoelectric equations

2.1 Model

A single degree of freedom model with structural stiffness, viscous damping and a piezo element is considered (figure 1). Different power harvesting circuits are considered and elaborated on where necessary. It is governed by the following equations:

$$M\ddot{u} + C_s\dot{u} + K_s u - \theta V_p = F(t) \tag{1a}$$

$$\theta\dot{u} + C_0\dot{V}_p = I(t) \tag{1b}$$

where K_s represents the structural stiffness including the short-circuited piezo element. The electro-mechanical coupling coefficient θ is calculated as $e_{33}A/L$ with e_{33} a piezo material constant, A the loaded cross-section and L the thickness of the element. The variables C_s, u, V_p, $I(t)$ and C_0 represent viscous damping, displacement, and piezo element voltage, current and capacitance respectively.

2.2 Motivation

The mechanical and electrical domains are coupled by θ in equations (1). Most electrical circuits such as DC impedance matching [9], synchronous electric charge extraction (SECE) [10], or synchronized switch harvesting on inductor (SSHI) [12] techniques introduce strong non-linearities in the voltage function, greatly increasing the mathematical complexity.

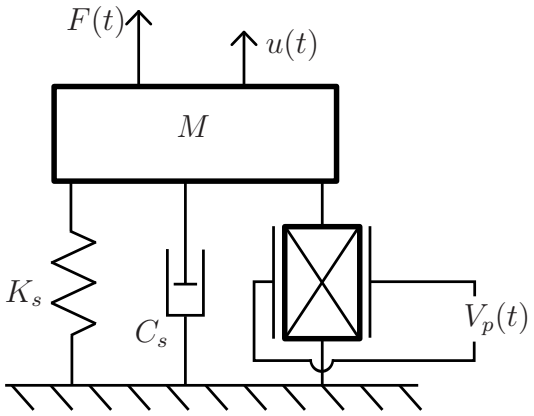

Figure 1. SDOF dynamic model

For weakly coupled systems (or low θ) the voltage term may generally be neglected in the mechanical domain, allowing for a linear calculation of the dynamics of the structure. Subsequently the electrical domain is solved based on the previously derived displacements.

For an optimization routine strong coupling (high θ) requires solving the full system of equations including non-linear terms leading to lengthy computations. A linear approximation to the non-linear equations which maintains accuracy is desirable. One goal of the *CleanSky* project is a single simulation environment encompassing aerodynamics, structural dynamics, etc. Inclusion of additional non-linear equations due to power harvesting greatly increases calculation time and may reduce numerical stability. It will be shown that structural damping provides a satisfactory alternative to the full equations.

2.3 Fundamental comparison

In [9, 10] expressions for the harvested power based on input frequency ω and peak displacement u_0 are presented. Equations (2a) and (2b) represent the power generated by DC impedance matching and SECE respectively. An optimized load is assumed for the former.

$$P = \frac{\theta^2 \omega u_0^2}{2\pi C_0} \tag{2a}$$

$$P = \frac{2\theta^2 \omega u_0^2}{\pi C_0} \tag{2b}$$

In a general sense $P = C_1 \omega u_0^2$, with C_1 determined by the circuit and piezo properties. From [14] the power dissipated by structural damping is found to be $P = (\alpha \omega u_0^2)/(2\pi)$ [1]. Clearly the power generated through harvesting and that dissipated by structural damping show similarities, for both: $P \propto \omega u_0^2$. Presuming this a single – and most important – linear equation of motion may be derived which governs piezo electric oscillators under sinusoidal excitations using a structural damping approach.

Structural damping can be included in a 1 DOF system in either of the following two ways [14]:

$$M\ddot{u} + \left(C_s + \frac{\alpha}{\pi\omega}\right)\dot{u} + K_s u = F(t) \tag{3a}$$

$$M\ddot{u} + C_s\dot{u} + K_s\left(1 + i\gamma\right)u = F(t) \tag{3b}$$

with α (unit *N/m*) representing the constant linking the amplitude with the energy dissipated per cycle, and γ ($\alpha/\left(\pi K_s\right)$) the equivalent structural damping factor.

[1] Note that in various literature both θ and α are used for the piezo electric force factor. θ is used here in order to reserve α for the structural damping coefficient as per [14]

The natural frequency of piezo augmented systems is dependant on the amount of coupling. Little coupling leads to a natural frequency of the mechanical system alone and high coupling leads to an increase in this frequency. The additional apparent stiffness induced by the voltage buildup across the piezo is lost in (3): $i\gamma$ is complex notation and relates to damping. In the following section an additional (real) term is determined to account for the added stiffness from voltage buildup. Subsequently, a numerical investigation for the SECE circuit is conducted to explore the limitations of this presumption.

2.4 Applied to impedance matching

The analytical solution for peak displacement u_0 in case of an impedance matching system can be found in [9]. Assuming an optimum resistance it reads as follows when normalized with the static displacement:

$$\bar{u}_0 = \frac{u_0 K_s}{F_0} = \frac{1}{\left(1 - \Omega^2 + \frac{1}{2}k_e^2\right) + i\left(2\zeta\Omega + \frac{k_e^2}{\pi}\right)} \tag{4}$$

with Ω, ζ and k_e^2 representing the dimensionless excitation frequency, mechanical damping and electromechanical coupling $\theta/(K_s C_0)$ as defined in [9]. Compared to a mechanical oscillator added damping and stiffness due to the piezo electric component are recognized as k_e^2/π and $k_e^2/2$ respectively.

The response of a structurally damped system is

$$\bar{u}_0 = \frac{1}{(1 - \Omega^2) + i(2\zeta\Omega + \gamma)} \tag{5}$$

Comparing (4) and (5) k_e^2/π is equivalent to the structural damping factor γ, or in case (3a) is used $k_e^2 K_s$ for α. The added stiffness from the electromechanical coupling is accounted for by adding $\frac{1}{2}\alpha$ or $\frac{1}{2}\gamma\pi$ in the stiffness term, yielding the following equation for the linearized approach to a piezoelectric oscillator using a DC impedance matching circuit:

$$M\ddot{u} + \left(C + \frac{\theta^2}{C_p \pi \omega}\right)\dot{u} + \left(K_s + \frac{\theta^2}{2C_p}\right)u = F(t) \tag{6}$$

Using this equation it is possible to perform calculations on systems experiencing sinusoidal loads, optimization routines, etc. Such an equation becomes more useful as the structure becomes more complex e.g.: high coupling and particularly for multiple patches . Also, undamped structures may initially exhibit strains too large for ceramics. An iteration scheme may then start with a patch located in a viable position after which the calculation will converge to locating the patch at the highest strain area, since coupling may attenuate the deformations.

2.5 Applied to Synchronous Electric Charge Extraction

In [10] equations only describe the behaviour of the system near resonance, where [9] provides a generally applicable equation. In light of the impedance matching approximation the same approach is investigated for the SECE circuit.

First the equivalent structural damping factor is determined from (2b): $\gamma = 4k_e^2/\pi$. The addition to the stiffness term is investigated using a *MATLAB-Simulink* model which represents the full mechanical and piezoelectric behaviour of the SECE circuit. A sinusoidal input force is imposed and the simulation is executed until a harmonic state is achieved.

A curve fit is performed on the results from the simulation where displacement magnitude is written as a function of dimensionless frequency. The function used in the fit process was defined as:

$$\bar{u}_0 = \frac{1}{\left(1 - \Omega^2 + C_2\right)^2 + \left(2\zeta\Omega + \frac{4k_e^2}{\pi}\right)^2} \tag{7}$$

The unknown C_2 was then determined by the fit process resulting in $C_2 = k_e^2$. The linearized normalized displacement and power equations then become

$$\bar{u}_0 = \frac{1}{\left(1 - \Omega^2 + k_e^2\right) + i\left(2\zeta\Omega + \frac{4}{\pi}k_e^2\right)} \tag{8a}$$

$$\bar{P} = \frac{2k_e^2\Omega}{\pi} \frac{1}{\left(1 - \Omega^2 + k_e^2\right)^2 + \left(2\zeta\Omega + \frac{4}{\pi}k_e^2\right)^2} \tag{8b}$$

Figure 2 compares the *Simulink* response and the linear approach of (7), with speed and response data normalized by the first natural frequency and static deflection respectively. The deviation at low relative speeds is discussed in section 3.2, after which the error quickly becomes negligible.

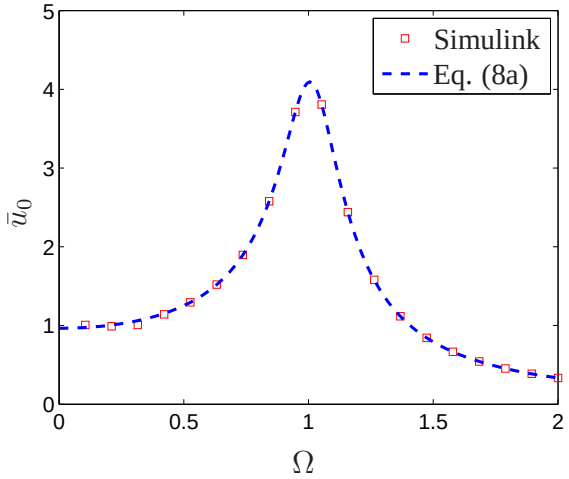

Figure 2. Simulink and fitted SECE response

Using these values the SECE equivalent to equation 6 becomes:

$$M\ddot{u} + \left(C_s + \frac{4\theta^2}{C_p\pi\omega}\right)\dot{u} + \left(K_s + \frac{\theta^2}{C_p}\right)u = F(t) \tag{9}$$

The factor 4 in the damping term reflects the higher energy dissipation of the SECE circuit over DC impedance matching. The additional apparent stiffness is twice that compared to (4), reflecting the higher voltage achieved by the SECE circuit. Mathematical derivation of the SECE system has not yet been performed in literature, currently equations (8a) and (8b) are therefore unproven. Derivation must be performed to confirm this linearization.

3. Investigation of validity for SECE

3.1 General discussion

The simplification presented is only valid under certain circumstances, most importantly a sinusoidal excitation. In light of the *Clean Sky* project, there is one clearly dominant frequency in the vibrations of a helicopter rotor blade.

A parameter study is done to investigate the boundaries of this linearization based on the SECE circuit of [10]. A Fourier series of two sine waves is used as input for the *Simulink* model. The electromechanical coupling k_e^2, damping ζ, force ratio F_0/F_1 (see equation (10)), phase ϕ and frequencies

ω_0 and ω_1 are varied. The various parameters are specified in table 1. The discussion is based on the error function given in equation (11), comparing (7) and the simulink data.

$$F(t) = F_0 \sin(\omega_0 t) + F_1 \sin(\omega_1 t - \phi) \tag{10}$$

$$Err = \frac{u_{0,linear} - u_{0,simulink}}{u_{0,simulink}} \tag{11}$$

Table 1. Parameter study values

Parameter	Value
k_e^2	0.01, 0.1
ζ	0.01, 0.1
F_0/F_1	0.01, 0.1, 1
ϕ	$(0, 1/2, 1, 3/2)\pi$

An example of a result is given in figure 3. The error function is plotted against normalized frequencies Ω_0 and Ω_1. Similar plots were made for all combinations of the parameters. Note that the error is capped at ± 0.5. The most important conclusions of the parameter study are:

- The relative phase does not significantly influence the results. Along the line $\Omega_0 = \Omega_1$, where the excitation becomes a single sine wave, are within a few percent error. Far from this line ϕ becomes irrelevant.
- The linearization induces less than 2% error on the displacement for $F_0/F_1 = 0.1$, and $k_e^2 = 0.01$ for the speeds investigated, near resonance the error increases to 10%.
- For high coupling $k_e^2 \gtrsim 0.1$ secondary discharges arise, see section 3.2 for further discussion.
- For $F_0/F_1 = 0.1$ and operating below resonance, the error increases to 20%. Above the secondary discharge threshold the linearization is within a few percent error.

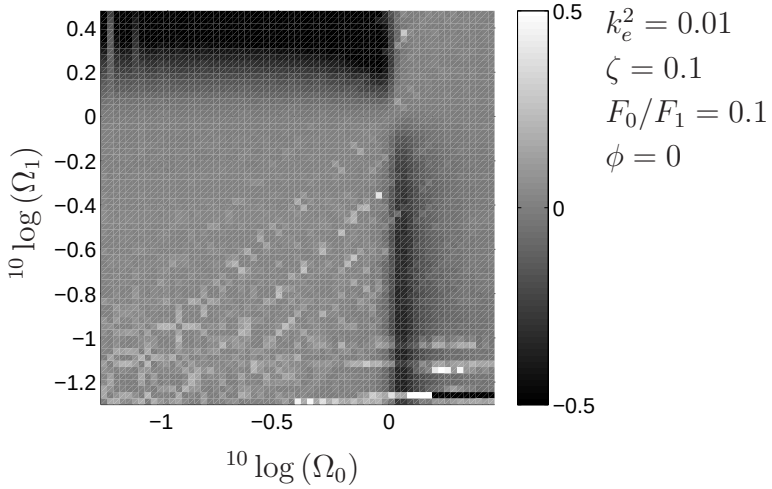

Figure 3. Typical error plot

Based on the simulation results the linearization is valid assuming the following conditions: $F_0/F_1 < 0.1$ and the system is either weakly coupled or the viscous damping to electromechanical coupling ratio is large.

In case of the helicopter rotor blade example vibration data shows the rotation speed to be dominant. Additionally the aerodynamics lead to large damping ratio's. The first out-of-plane mode exhibits $\zeta \approx 0.4$ and for the first in-plane mode $\zeta \approx 0.2$. The linear approximation of power harvesting presented here is a promising linearization in a full dynamic blade model.

3.2 Discharge induced oscillations

Cases with high coupling exhibit a very erratic error which is caused by discharging of the piezo patch. This effect is strengthened when the viscous damping is decreased. Upon discharge of the piezo patch using the SECE circuit a quick drop in voltage occurs and through electro-mechanical coupling a drop in the force exerted by the piezo element is achieved. The duration of this ramp depends on the natural frequency of the capacitor-inductor loop of the circuit ω_{LC}.

Typically a quick discharge is desired to maximize harvesting efficiency where during a slow discharge significant displacement occurs, reducing efficiency. These undesired discharges occur under the following conditions: high coupling, low damping, $\Omega \ll 1$ and $\omega_{LC} \gtrsim \omega_{sc}$. From the *Simulink* results there typically seems to be a distinct frequency boundary beneath which the discharges occur. This boundary increases with higher coupling.

Figure 4 shows the excitation force, displacement and associated voltage as calculated by *Simulink*. Here $\Omega \approx 0.3$, $k_e^2 = 0.1$ and $\zeta = 0.035$. Near the first displacement peak a discharge is triggered which is clearly visible from the voltage curve, causing a large change in net force. As the excitation force is still increasing the mass continues in the same direction. The discharging adds a secondary vibration at the natural frequency which after a few cycles accumulates enough phase difference to trigger a new undesired discharge (the last peak shown). Increasing viscous damping while maintaining the excitation frequency will suppress this effect. From error plots similar to figure 3 it appears that this effect only occurs for the major force (F_1, Ω_1) when $F_0/F_1 \ll 1$. Error plots similar to figure 3 also indicate a frequency threshold below which this will occur.

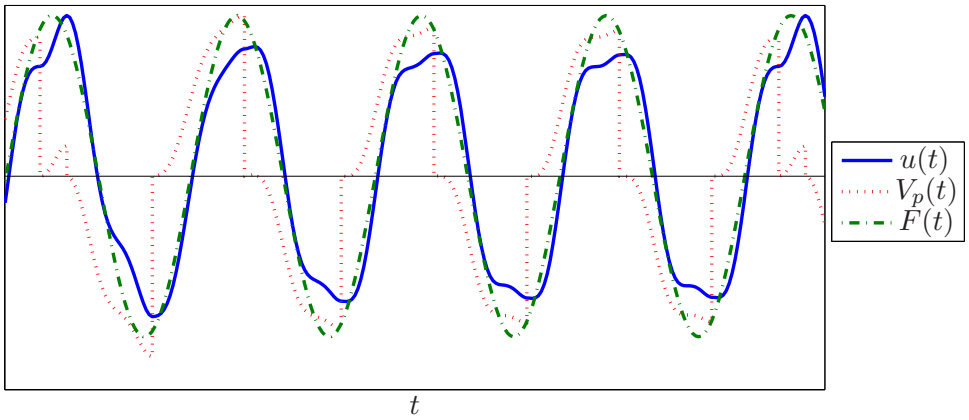

Figure 4. Additional discharges due to high coupling

Despite the sinusoidal force the displacement in these cases is far from sinusoidal, imposing operational limitations on the system presented by [10]. This effect is relevant for all circuits which induce swift voltage changes (such as SSHI [12]) and meet the requirements listed previously. This limits the use of analytical solutions assuming sinusoidal motion. From an implementation standpoint [11] presents a method which can be used to filter small local extrema from large global ones, negating the large losses associated with these small discharges.

For impedance matching these extra oscillations are non-existent: there are no swift voltage changes other than what is induced by mechanical straining of the element. In this respect the linear approach should present a more consistent approximation. The difficulty with the impedance matching approximation will lie in intermittent conduction due to local versus global maxima. For displacement signals with one dominant frequency there is again no problem. With 2 frequency components such as used to investigate the SECE circuit, similar force levels will disrupt the approximation. This has not yet been investigated.

4. Conclusion

A linearization of the equations of motion of piezo augmented dynamic systems is presented for two power harvesting circuits: DC impedance matching and synchronous electric charge extraction. Global mechanical behaviour is preserved while details of the electrical domain are lost. Peak voltage and harvested power however can be calculated in post-processing.

For impedance matching the linearization is derived from a complete analytical solution based on sinusoidal excitation, providing a mathematical basis. Therefore it is valid for all situations where predominantly sinusoidal excitations are considered. Practical confirmation remains to be done.

For the SECE circuit validity of the linearization has been investigated using a simulated model. It can be applied to systems with sinusoidal excitations with some allowance for minor additional vibrations. Strong coupling, low viscous damping and operation well below resonance leads to additional self-induced vibrations, reducing accuracy. This is suppressed with additional viscous damping.

REFERENCES

[1] J. Feenstra, J. Granstrom, and H. Sodano. Energy harvesting through a backpack employing a mechanically amplified piezoelectric stack. *Mech Syst Signal Pr*, 2007.

[2] S. W. Arms. Energy harvesting, wireless, strain sensor for damage tracking of helicopter components. In *Third European Workshop on Structural Health Monitoring*, 2006.

[3] H. Sodano and D. J. Inman. Generation and storage of electricity from power harvesting devices. *J Intel Mat Syst Str*, 2005.

[4] D. Shen, S. Choe, and D. Kim. Analysis of piezoelectric materials for energy harvesting devices under high-g vibrations. *Jpn J Appl Phys*, 2007.

[5] H. A. Sodano, J. Lloyd, and D. J. Inman. An experimental comparison between several active composite actuators for power generation. *Smar Mat St*, 2006.

[6] G. K. Ottman, H. F. Hofmann, A. C. Bhatt, and G. A. Lesieutre. Adaptive piezoelectric energy harvesting circuit for wireless remote power supply. *IEEE T Power Electr*, 2002.

[7] G. K. Ottman, H. F. Hofmann, and G. A. Lesieutre. Optimized piezoelectric energy harvesting circuit using step-down converter in discontinuous conduction mode. *IEEE T Power Electr*, 2003.

[8] H. Kim, S. Priya, H. Stephanou, and K. Uchino. Consideration of impedance matching techniques for efficient piezoelectric energy harvesting. *IEEE T Ultrason Ferr*, 2007.

[9] Y C Shu and I C Lien. Efficiency of energy conversion for a piezoelectric power harvesting system. *J Micromech Microeng*, 2006.

[10] E. Lefeuvre, A. Badel, C. Richard, and D. Guyomar. Piezoelectric energy harvesting device optimization by synchronous charge extraction. *J Intel Mat Syst Str*, 2005.

[11] M. Lallart, E. Lefeuvre, C. Richard, and D. Guyomar. Self-powered circuit for broadband, multimodal piezoelectric vibration control. *Sensor Actuat A-Phys*, 2007.

[12] D. Guyomar, A. Badel, E Lefeuvre, and C. Richard. Toward energy harvesting using active materials and conversion improvement by nonlinear processing. *IEEE T Ultrason Ferr*, 2005.

[13] Y. B. Jeon, R. Sood, J. h. Jeong, and S.-G. Kim. Mems power generator with transverse mode thin film pzt. *Sensor Actuat A-Phys*, 2004.

[14] L Meirovitch. *Fundamentals of Vibrations*. McGraw Hill, 2001.